

Appendix M
Socket Laboratory Analysis

1.0 Introduction..... 1

2.0 Sockets Analyzed 1

2.1 M4N_T Socket (WJE-NESC).....1

2.2 Other Sockets (TT-Socotec)2

3.0 Cable Slips..... 5

4.0 Longitudinal Cuts and Macroetch 6

5.0 Radiography..... 8

6.0 Transverse Cuts and Wire Brooms10

7.0 Zinc Properties16

7.1 Composition16

7.2 Tensile Properties17

7.3 Grain Size19

8.0 Miscellaneous21

8.1 No-Shoulder Socket Design21

8.2 Wire Galvanizing Layer22

1.0 Introduction

The cables of the telescope were terminated with zinc-filled spelter sockets, which are commonly used to connect large structural cables. The first and second cable failures in 2020 occurred near or within the sockets at the top of Tower 4, and significant cable slips were observed on other sockets before and after the cable failures. The behavior and failure of the sockets is therefore a focus of our investigation, and several sockets were recovered from the collapsed structure and analyzed in laboratories. The results of the laboratory analyses are presented in this appendix, which is organized by type of laboratory test.

2.0 Sockets Analyzed

Six of the telescope's sockets were analyzed in laboratories, including the two sockets that failed before the collapse and four other sockets selected based on cable slip and access in the early stages of site cleanup. The sockets considered and the cable slip observed at each socket are shown in Figure 1.

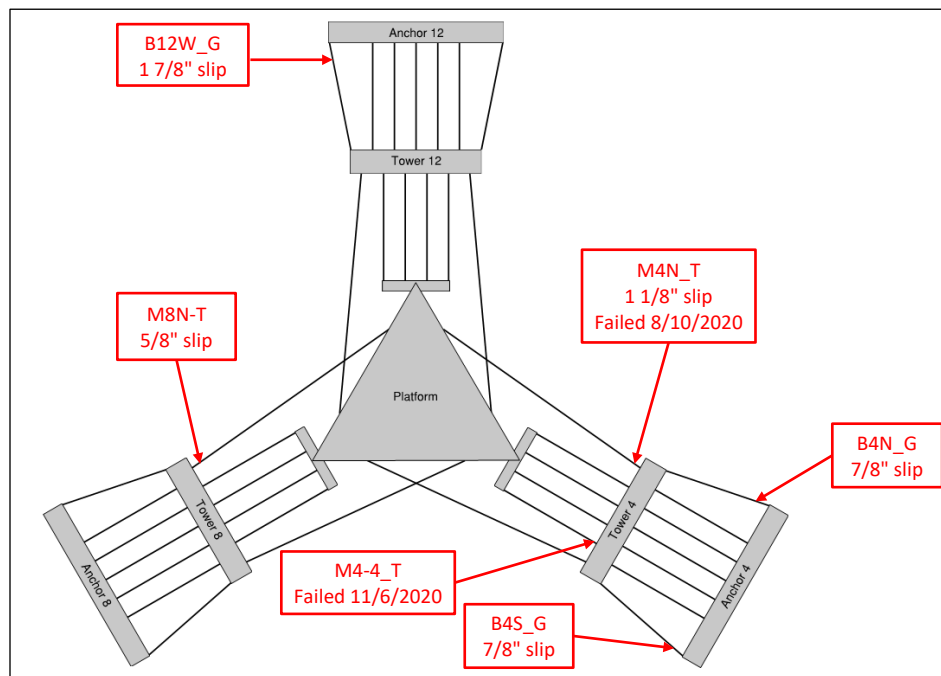


Figure 1: Map of sockets analyzed.

2.1 M4N_T Socket (WJE-NESC)

Socket M4N_T is where the first cable failure occurred on August 10, 2020. The socket was recovered from the top of tower 4 on September 23, 2020 (Figure 2), and shipped to Kennedy Space Center for analysis by the NASA Engineering and Safety Center (NESC) in collaboration with Wiss, Janney, Elstner Associates (WJE). The cable end that pulled out of M4N_T was recovered after the collapse (Figure 3) and also analyzed by WJE-NESC. The results of the WJE-NESC analysis are provided in a report,¹ and we include some of the report's findings in this appendix as additional data points when comparing the properties and behavior of different sockets.

¹ Wiss, Janney, Elstner Associates (WJE). *Auxiliary Main Cable Socket Failure Investigation*. June 21, 2021. Draft report provided by WJE.



Figure 2: Socket M4N_T recovered from Tower 4 after M4N failure (photo: WJE).



Figure 3: Cable end pulled out of socket M4N_T.

2.2 Other Sockets (TT-Socotec)

We selected five additional sockets for laboratory analysis:

- M4-4_T (Figure 4), where the second cable failure occurred on November 6, 2020.
- B12W_G (Figure 5), which exhibits the largest cable slip (1.875 inch).
- M8N_T (Figure 6), which exhibits a relatively small cable slip (0.625 inch).
- B4N_G (Figure 7) and B4S_G (Figure 8), which exhibit intermediate cable slips (0.875 inch)

We worked with Socotec (formerly Lucius Pitkin Inc) to analyze these five sockets in Socotec's New York, NY laboratory. Except for the failed socket M4-4_T, each socket was shipped to Socotec with a segment of cable still attached. Pictures of the five sockets as received by Socotec are provided in Figure 4 to Figure 8.

Unless socket M4N_T is mentioned, the methods and results presented in this appendix apply to the five sockets listed above and analyzed by Socotec.



Figure 4: Socket M4-4_T (photos: Socotec).



Figure 5: Socket B12W_G (photos: Socotec).



Figure 6: Socket M8N_T (photos: Socotec).

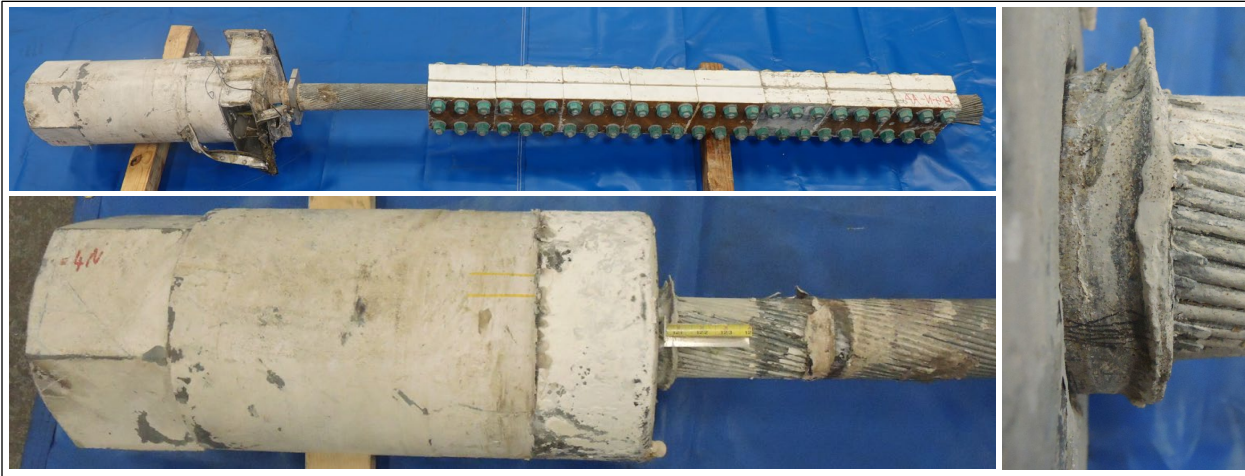


Figure 7: Socket B4N_G (photos: Socotec).

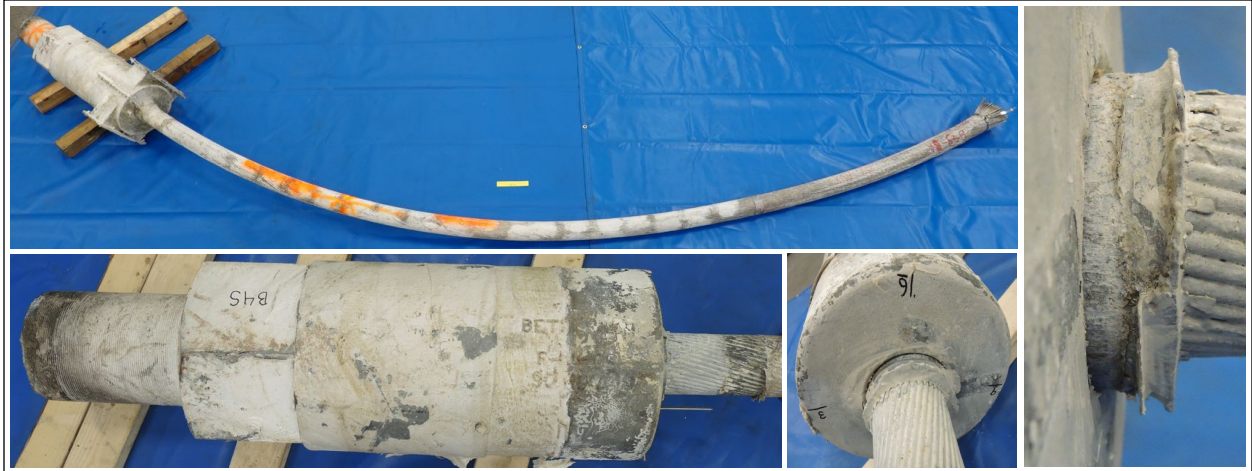


Figure 8: Socket B4S_G (photos: Socotec).

3.0 Cable Slips

The cable slip is the distance that a cable end shifted with respect to its socket, as measured outside of the socket. As shown in Figure 9, the cable slip can be measured as the length of zinc that was extruded out of the socket as the cable slipped. The cable slips at the sockets considered in laboratory studies are summarized in Table 1.

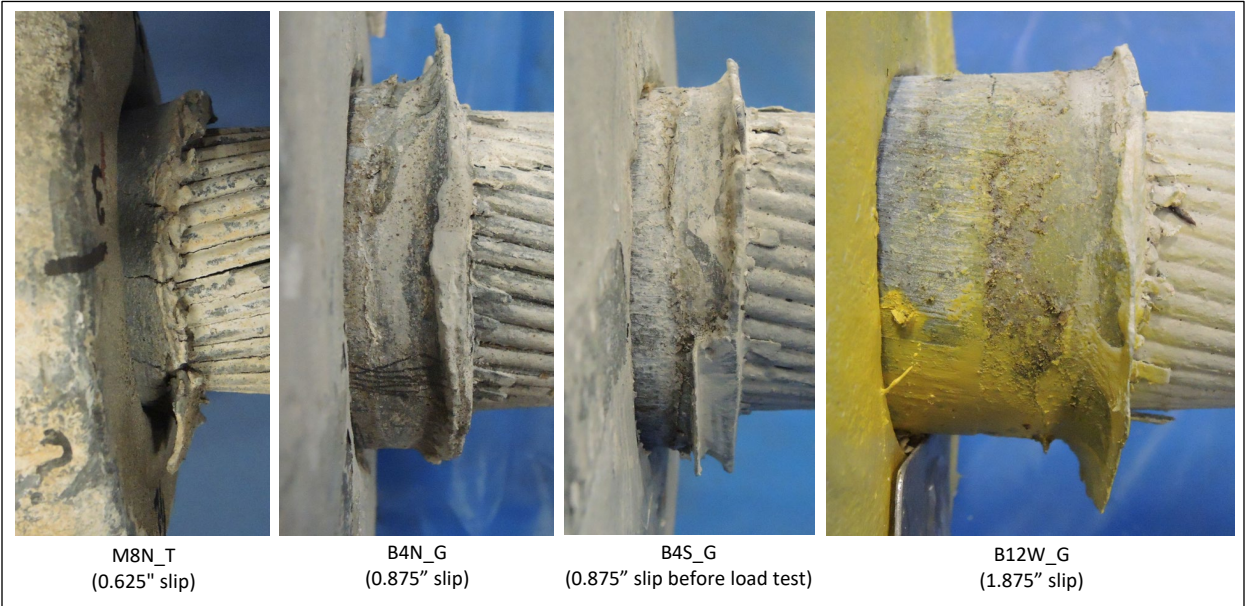


Figure 9: Cable slips observed on four auxiliary sockets (photos: Socotec).

Table 1: Cable slip of sockets considered in laboratory studies.

Socket	Cable slip	Notes
M4-4_T	Unknown	Not measurable before socket failure on November 6, 2020.
M4N_T	1.125	Measured on February 18, 2019. Socket failed on August 10, 2020.
M8N_T	0.625	Measured after collapse.
B4N_G	0.875	Measured on September 23, 2020, and after collapse.
B4S_G	0.875	Measured after collapse.
B12W_G	1.875	Measured on September 18, 2020, and after collapse.

4.0 Longitudinal Cuts and Macroetch

Each socket is a volume of cast steel with a cavity containing a zinc casting where the cable end is embedded. The steel of the sockets did not show any sign of damage or distress, and therefore the laboratory analysis focused on the zinc castings and embedded wires. To extract the zinc casting from each socket, the cast steel was sectioned and removed in steps as shown in Figure 10. After cutting away most of the socket's steel, two longitudinal cuts were made 180 degrees apart and the steel pieces were separated from the zinc casting by driving a wedge into one or both cuts.

After visual observation and measurements of the outside of the zinc casting, the first step to look inside the casting was to make a longitudinal cut. One of the cut surfaces was then macro-etched using hydrochloric acid. The macro-etched surfaces are shown in Figure 11 and key observations are as follows:

- The back surface of every casting is deformed, with a dip towards the socket's axis.
- In the castings of sockets B4S_G (failed during load test), B12W_G (maximum cable slip) and M4-4_T (failed on November 6, 2020), fracture planes developed at the back of the casting and a central core shifted in the direction of the cable pull.
- In the casting of socket B12W_G (maximum cable slip), several wires slipped with respect to the zinc outside of the displaced core.
- In the casting of M4-4_T (failed on November 6, 2020), several wires fractured inside the casting.

The core displacement and the fractured and slipped wires observed in the castings are relevant to the socket's failure modes and are further discussed in Appendix O.



Figure 10: Initial processing of socket B12W_G (photos: Socotec).

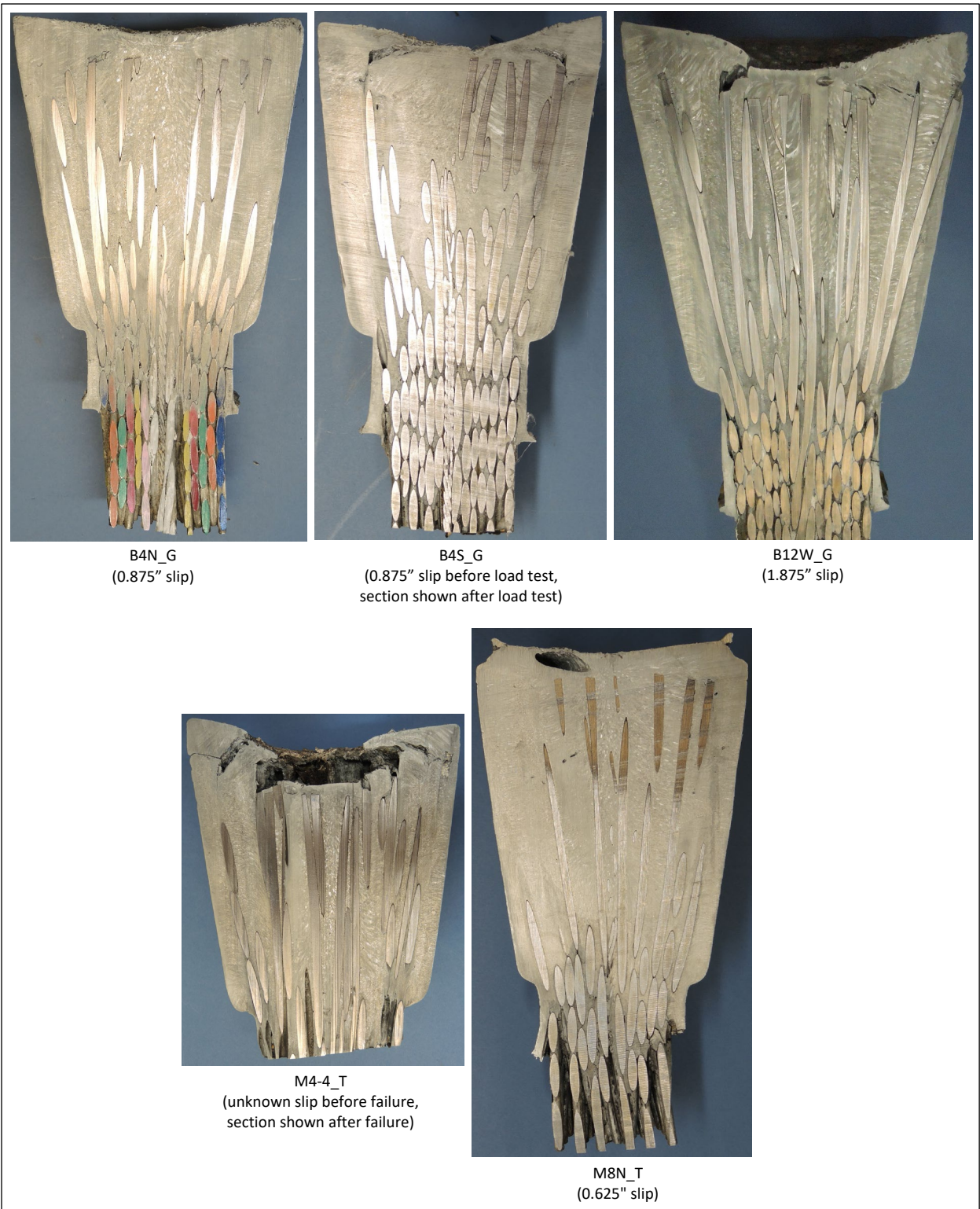


Figure 11: Macro-etched transverse sections of socket zinc castings (photos: Socotec).

5.0 Radiography

The largest cable slip was observed on socket B12W_G, and the longitudinal sectioning of that socket's zinc casting revealed that several cable wires had slipped within the casting. To determine the extent of the wire slips, we performed a neutron radiography of a one inch-thick longitudinal slice of the casting (Figure 12). The radiograph is shown in Figure 13 and reveals that within the slice considered, every wire end located outside of the displaced casting core has slipped. The wire slip distances varies from 0.4 to 0.8 inch. For comparison, we performed the same radiography on a one inch-thick slice of casting of socket M8N_T, which exhibits the smallest cable slip among the sockets considered in the laboratory studies. The radiograph is shown in Figure 14, and we observe a wire slip on only two wires, with a slip distance of less than 0.05 inch.

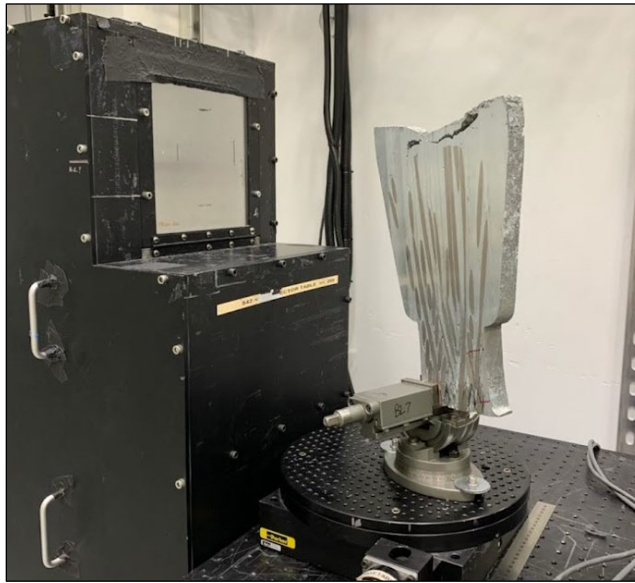


Figure 12: one inch-thick slide of B12W_G (1.875" slip) casting held in neutron imaging scanner
(photo: Adrian Brügger, Columbia University - Oak Ridge National Laboratory).

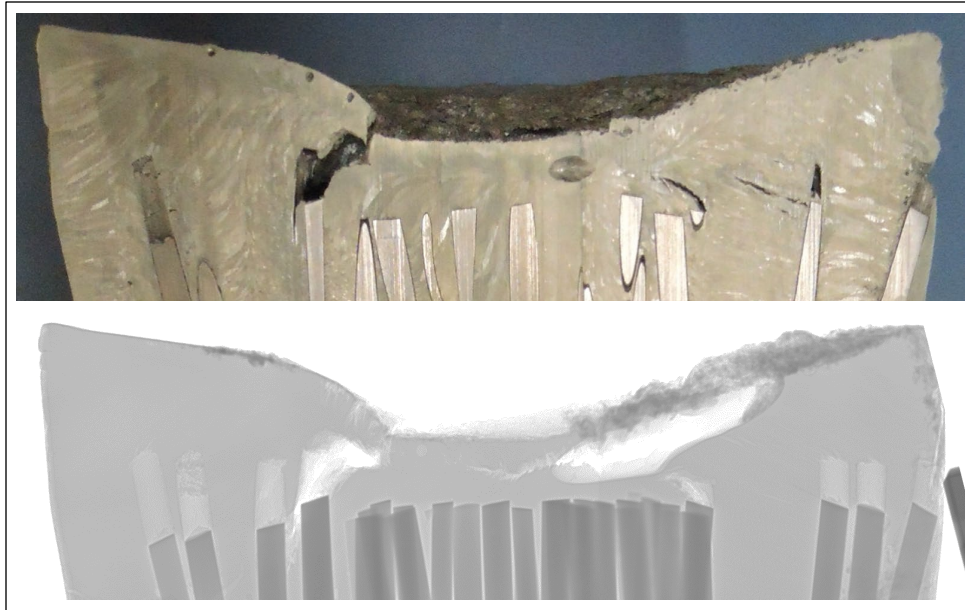


Figure 13: Neutron imaging of back of one inch-thick slice of B12W_G (1.875" slip) casting
(top photo: Socotec; bottom radiograph: Adrian Brügger, Columbia University - Oak Ridge National Laboratory).

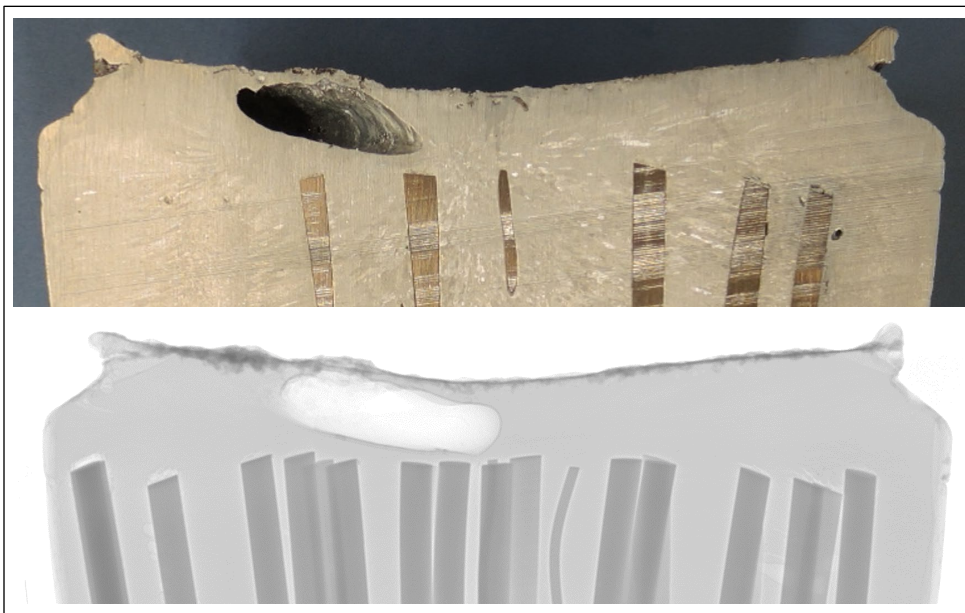


Figure 14: Neutron imaging of back of one inch-thick slice of M8N_T (0.625" slip) casting
(top photo: Socotec; bottom radiograph: Adrian Brügger, Columbia University - Oak Ridge National Laboratory).

6.0 Transverse Cuts and Wire Brooms

The zinc castings were sectioned in the transverse direction to observe the wire distribution within the casting, which is referred to as the wire broom. As shown in Figure 15, in some of the castings the wires were traced through multiple transverse sections and color-coded based on the layer that they belonged to in the cable.

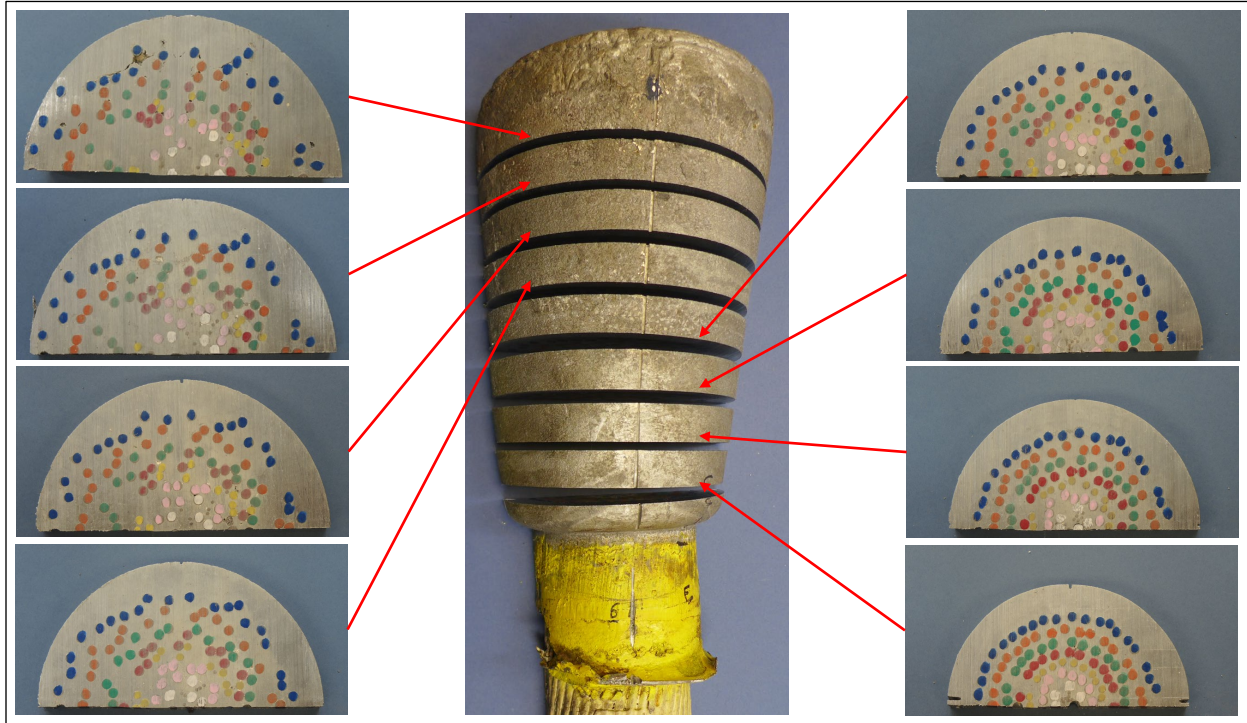


Figure 15: Transverse sections and wire layer tracing in B12W-G (1.875" slip) zinc casting (photos: Socotec).

Key transverse sections for the six sockets considered in the laboratory studies are shown in Figure 16 to Figure 21. For four of the sockets (M4-4_T, M8N_T, B4N_G and B12W_G), only one half of the casting was sectioned as the other half was preserved for other laboratory tests.

In every socket considered, the wire broom is irregular and does not follow any consistent pattern. General differences are immediately visible between the wire brooms in the sections close to the wire ends. For instance, most of the outer layer of wires is fully broomed out in socket M8N_T (Figure 17), while no wire is fully broomed-out in socket B12W_G (Figure 19). Then, the wire broom of M4-4_T (Figure 16) appears to be relatively uniform, while there is a significant zinc area with no embedded wire in socket B4N_G (Figure 18).

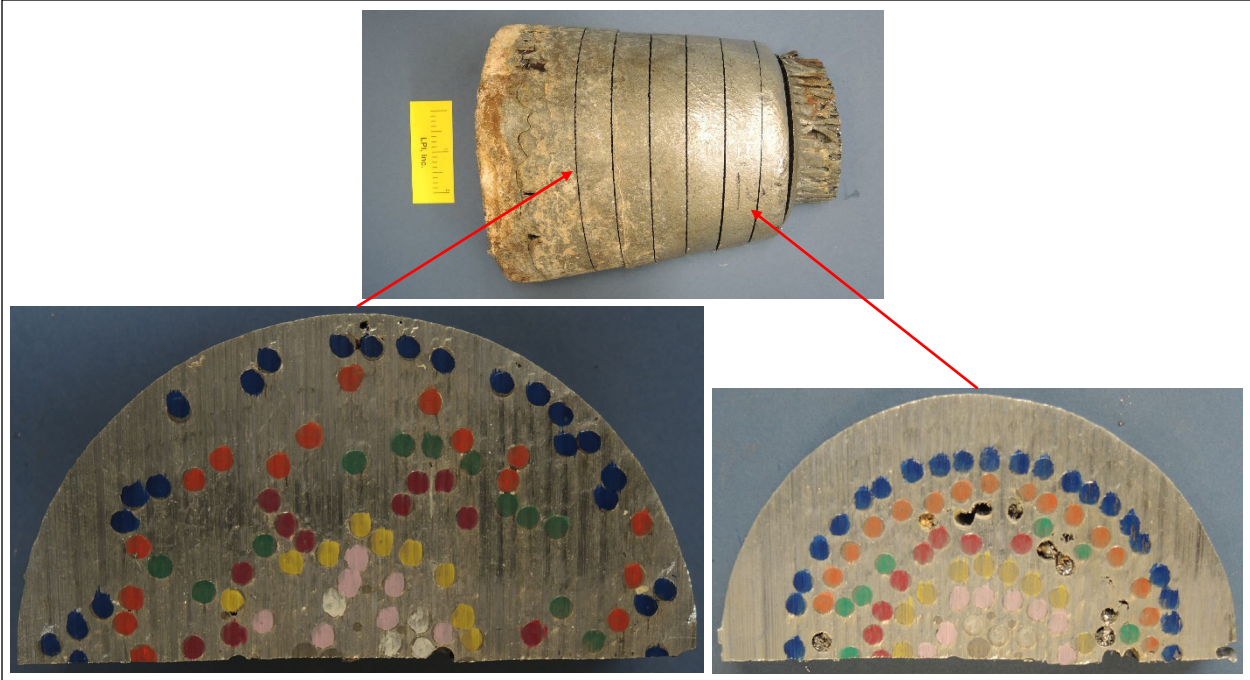


Figure 16: M4-4_T transverse sections (photos: Socotec).

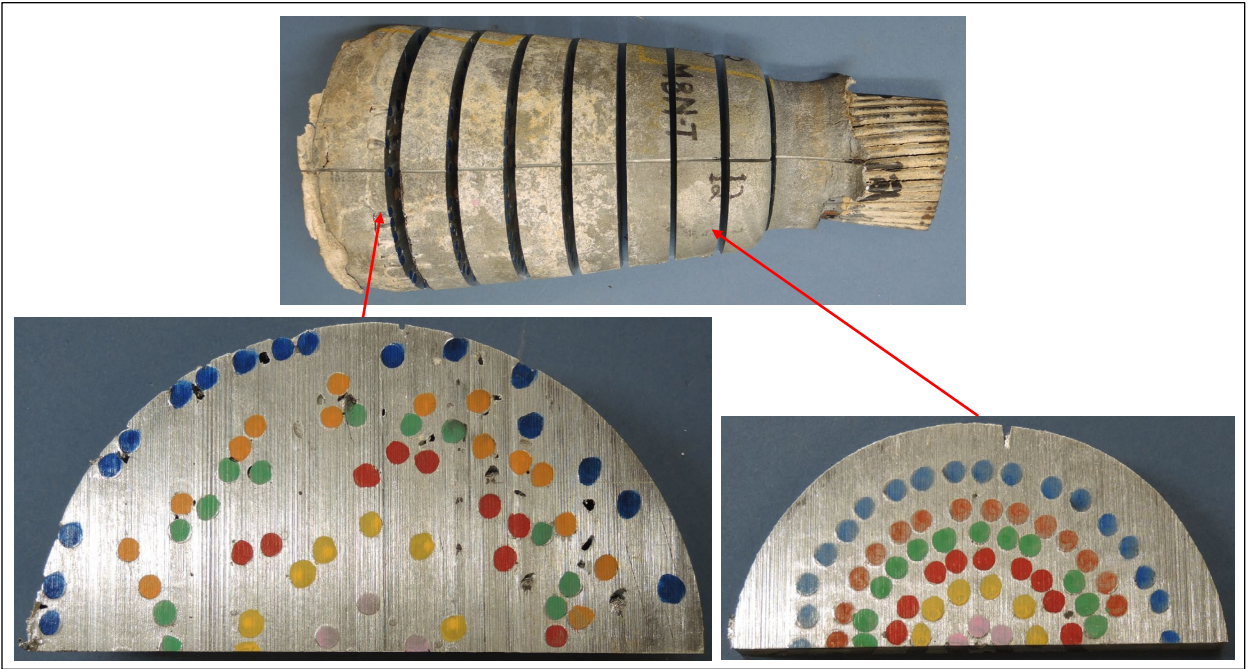


Figure 17: M8N_T (0.625" slip) transverse sections (photos: Socotec).

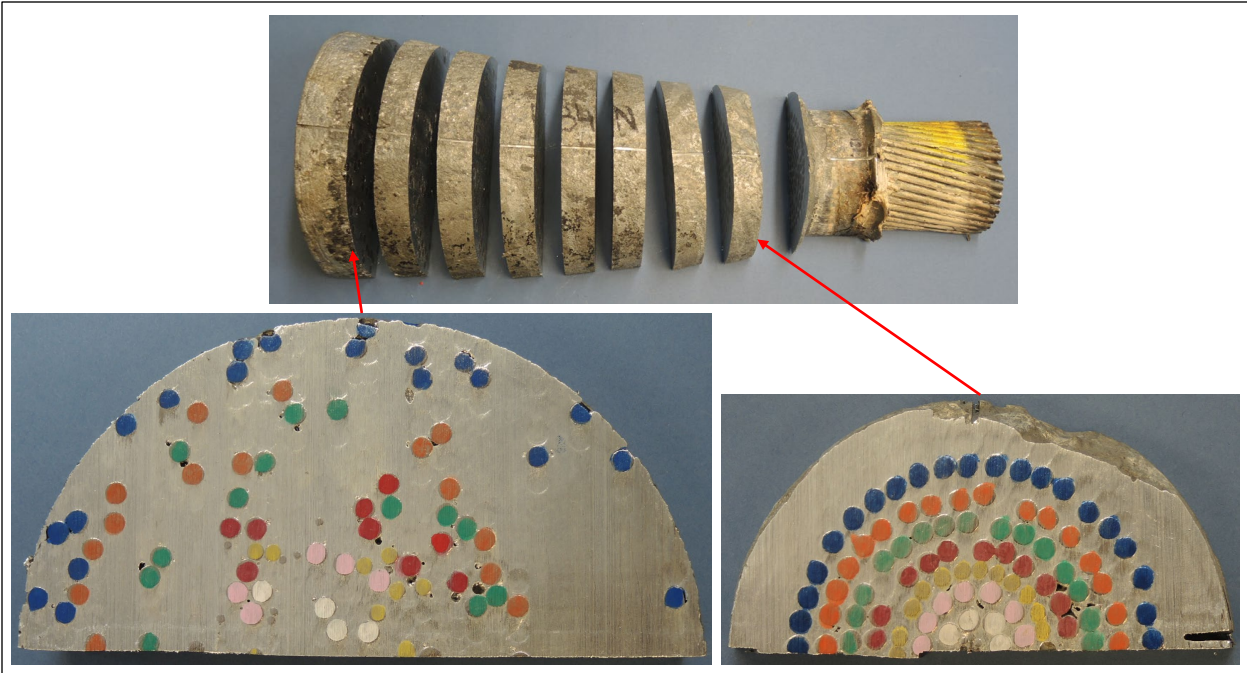


Figure 18: B4N_G (0.875" slip) transverse sections (photos: Socotec).

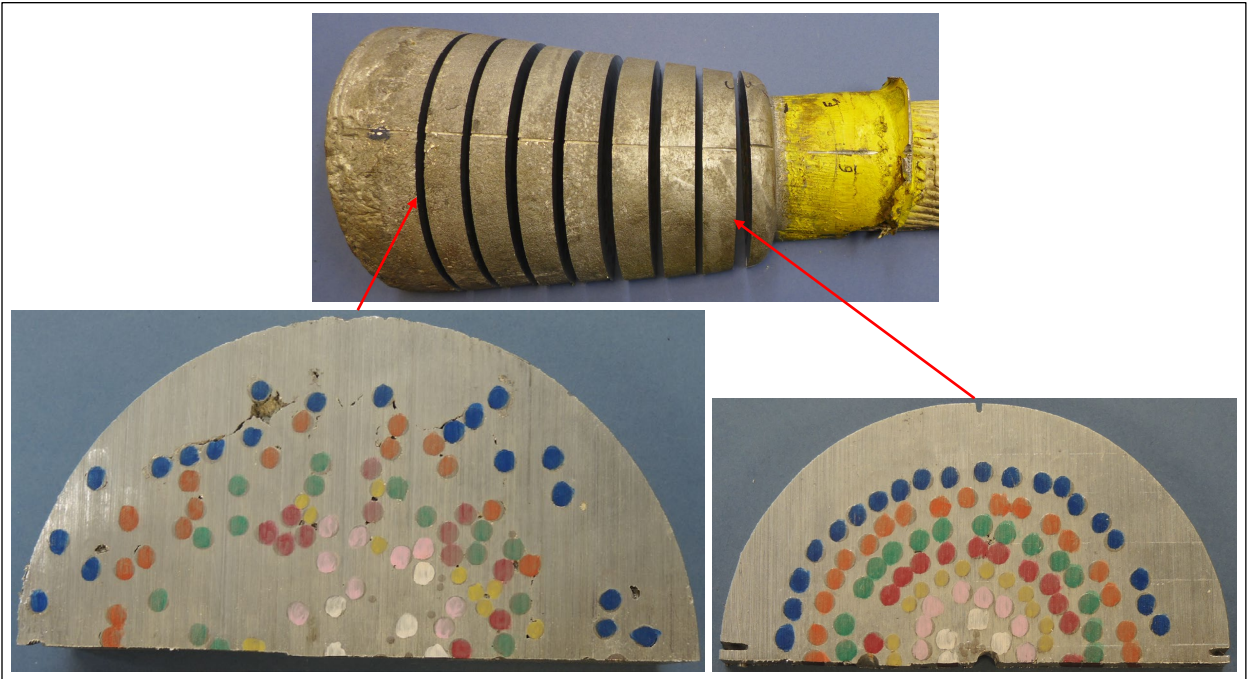


Figure 19: B12W_G (1.875" slip) transverse sections (photos: Socotec).

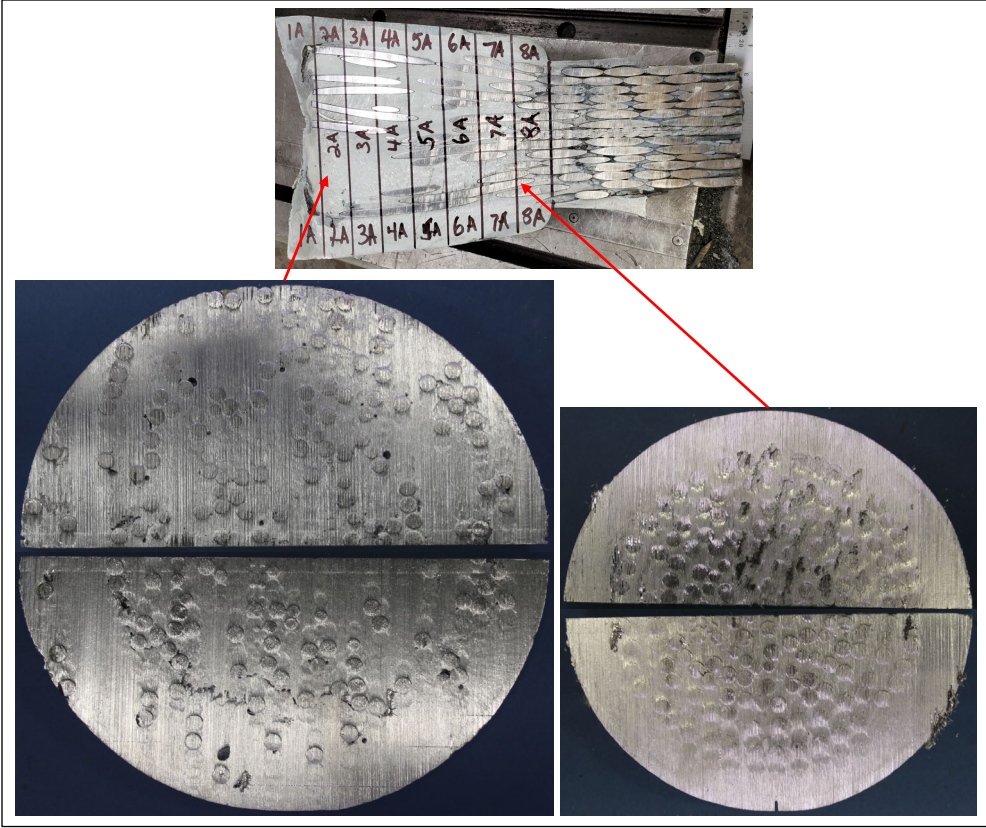


Figure 20: B4S_G (0.875" slip) transverse sections (photos: Socotec).

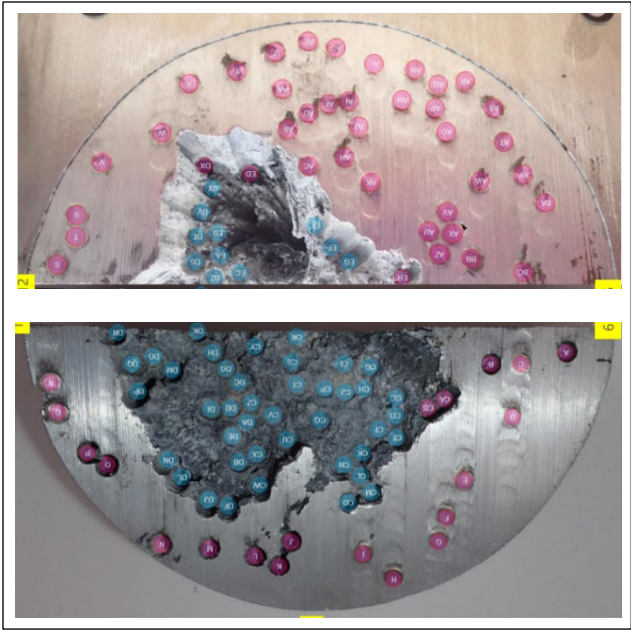


Figure 21: Wire locations at back of M4N_T (1.125" slip) (photos: WJE²).

² Wiss, Janney, Elstner Associates (WJE). *Auxiliary Main Cable Socket Failure Investigation*. June 21, 2021. Draft report provided by WJE.

The wire end distribution are shown in Figure 22 for the six socket castings considered. When the broom was observed on only half of the casting, the wire distribution was mirrored in the other half. For each type of socket, the actual brooms are compared to a hypothetical uniform broom where the wires are evenly-spaced in the radial and circumferential directions.

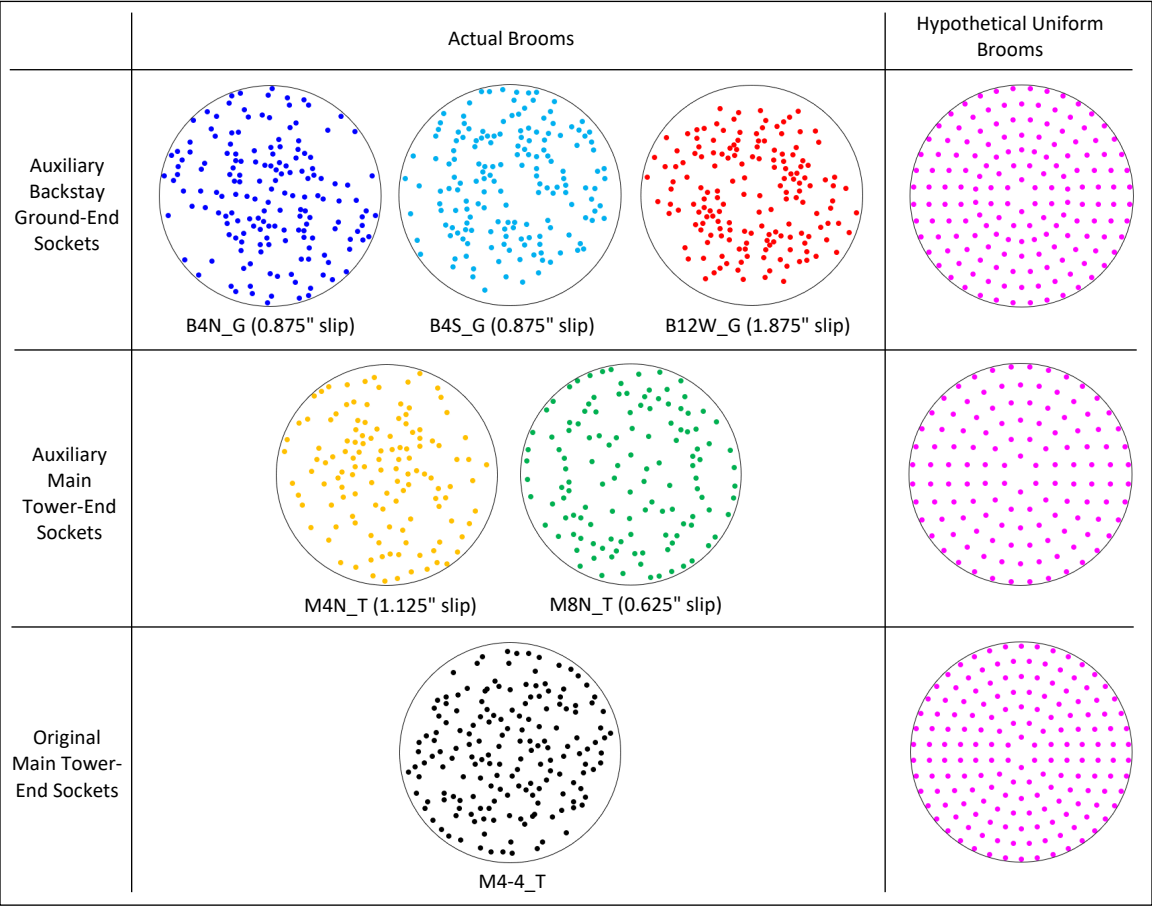


Figure 22: Wire end distribution at back of actual brooms and in hypothetical uniform brooms.

To compare the wire brooms quantitatively, we define a wire's brooming ratio and the wire's distance to the socket axis divided by the casting's radius at the wire ends (Figure 23). In a socket, the average brooming ratio is the average of the brooming ratios of all the wires.

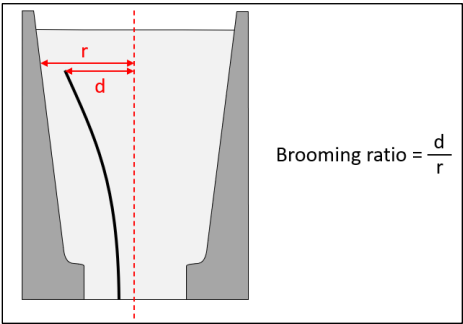


Figure 23: Definition of wire brooming ratio.

For the five sockets whose cable slips are known, the average brooming ratio is plotted against cable slip in Figure 24. We observe a general correlation, with the cable slip decreasing as the brooming ratio increases. Due to the limited number of data points, this correlation is not sufficient to draw a conclusion on the impact that the wire broom many have on the cable slips. The potential ties between wire broom and cable slip were further investigated through calculations presented in Appendix O. We also observe that socket M8N_T, which exhibits the smallest cable slip, is the only socket whose average brooming ratio is similar to the ones of the uniform brooms.

The cumulative distribution of the wire brooming ratios in each socket and in the uniform brooms are shown in Figure 25. For the uniform brooms, the distribution has discontinuities because the wires ends are assumed to remain in concentric layers.

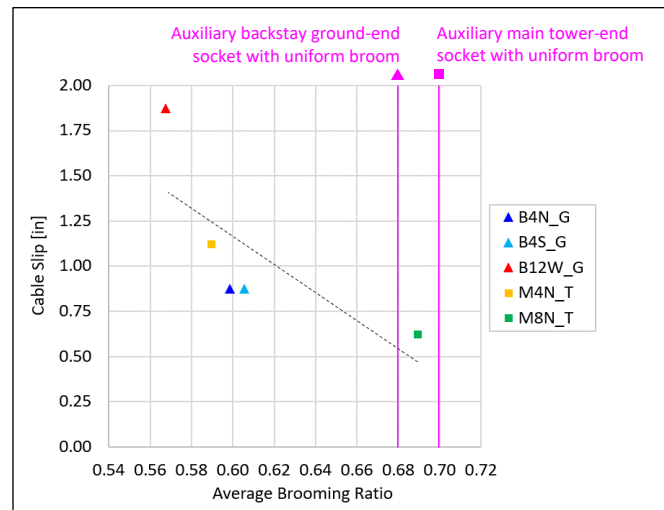


Figure 24: Wire average relative distance to center vs. cable slip.

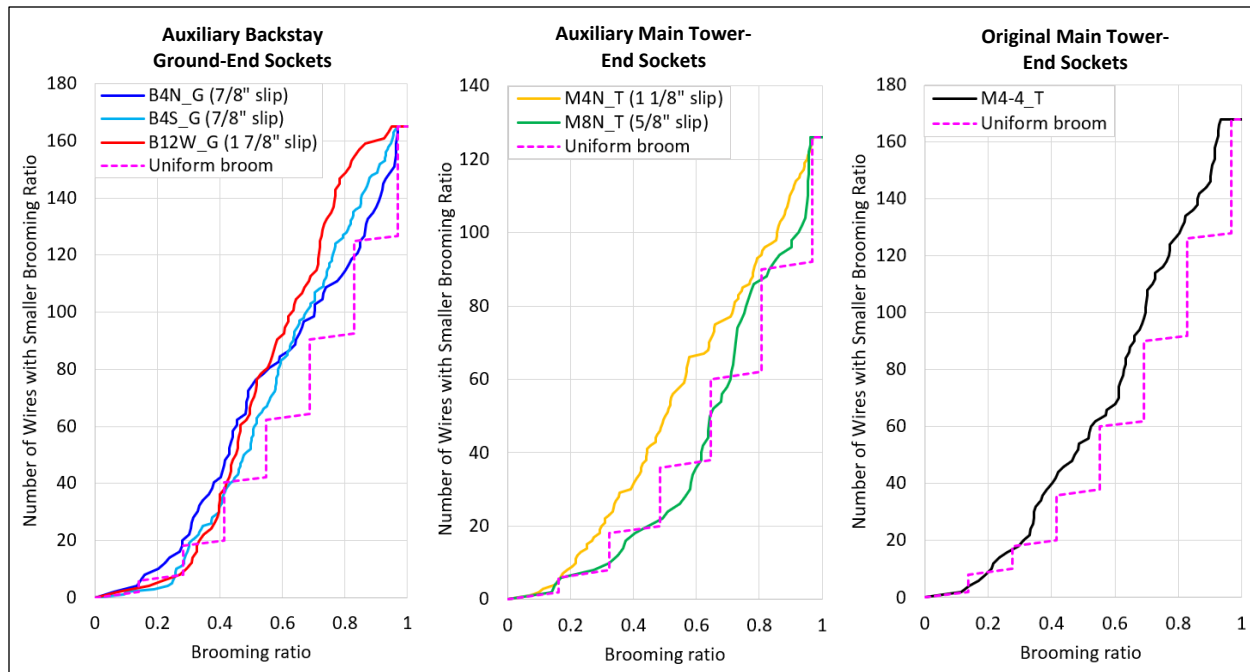


Figure 25: Cumulative distribution of wire brooming ratios.

7.0 Zinc Properties

7.1 Composition

The chemical composition of the zinc casting was tested through optical emission spectroscopy (OES) for one original and two auxiliary sockets. The results are shown in Table 2 and indicate that the three samples meet the high-grade requirements of the ASTM B6 standard.³ The ASTM B6 standard for high-grade requires the zinc to be 99.5 percent pure and was prescribed for the socket castings in the structural drawings of the original structure. We did not find any similar requirement in the construction documents of the upgraded structure, but the composition tests indicate that the sockets installed during the second upgrade also used pure zinc.

Table 2: Zinc composition by element weight.

Element	ASTM B6 High-Grade Limits		Arecibo Socket Samples		
	Min	Max	B4N_G	B12W_G	M4-4_T
Al		0.01%	< 0.01%	< 0.01%	< 0.01%
Cd		0.01%	< 0.01%	< 0.01%	< 0.01%
Cu		0.20%	< 0.01%	< 0.01%	< 0.01%
Fe		0.05%	0.01%	0.04%	0.02%
Mg			< 0.001%	< 0.001%	< 0.001%
Mn			0.001%	0.002%	0.005%
Ni			0.005%	0.005%	0.001%
Pb		0.45%	< 0.01%	< 0.01%	< 0.01%
Sb			< 0.001%	< 0.001%	< 0.001%
Sn			0.004%	0.003%	0.003%

³ American Society for Testing and Materials (ASTM). *ASTM B6-18. Standard Specification for Zinc*. 2018.

Total Non-Zn	0.5%	< 0.1%	< 0.1%	< 0.1%
Zn	99.5%	100.0%	99.9%	99.9%
	Meets ASTM B6 High Grade?	Yes	Yes	Yes

7.2 Tensile Properties

The ASTM B6 standard prescribed for the original cable sockets only covers the zinc's chemical composition, and it does not set any requirement on the zinc's mechanical properties. However, we performed a series of tensile tests to evaluate the mechanical behavior of the socket's zinc and their potential impact on cable slip and socket failure.

Ten miniaturized flat tensile specimens were machined from four socket castings. As shown in Figure 26, specimens were taken from the front (smaller diameter end) and back (larger diameter end) of each casting. The specimens had nominal cross-sectional dimensions of 0.2-inch x 0.2-inch, with a 0.625-inch gage length (Figure 27). Each specimen was tested at room temperature per ASTM E8. The specimens were taken from various locations of the casting.

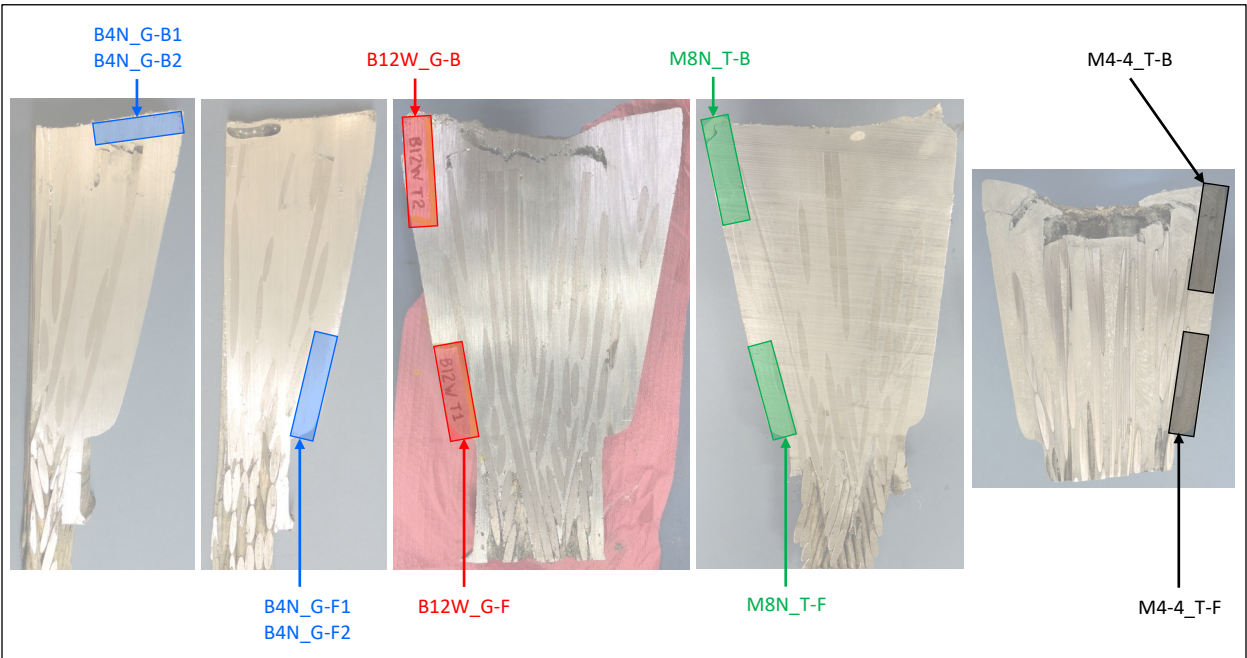


Figure 26: Tensile test sample locations in socket zinc castings (photos: Socotec).

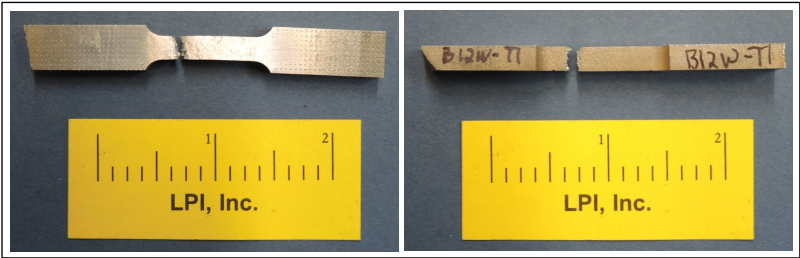


Figure 27: Zinc sample B12W_G-F after tensile testing to failure (photos: Socotec).

The results of the tensile tests are presented in Figure 28 as stress-strain curves up to the ultimate tensile stress reached. We first observe a wide range of ultimate tensile stress across the specimens, between three kilopound per square inch (ksi) and 12 ksi. The ultimate tensile stress is also reached for a wide range of strains. For every casting, the ultimate tensile stress is higher in the specimen(s) taken from the front of the casting than the specimen(s) taken from the back. This is consistent with the larger grain sizes observed at the back of the sockets, as described in (section 7.3 below).

For the three sockets whose cable slips are known, the tensile test results (yield stress, ultimate tensile stress, and strain at ultimate tensile stress) are plotted against cable slip in Figure 29. WJE-NESC performed tensile tests on the zinc of socket M4N_T, and the results provided in their report are added to the plots. We observe no correlation between cable slip and the tensile properties of the zinc.

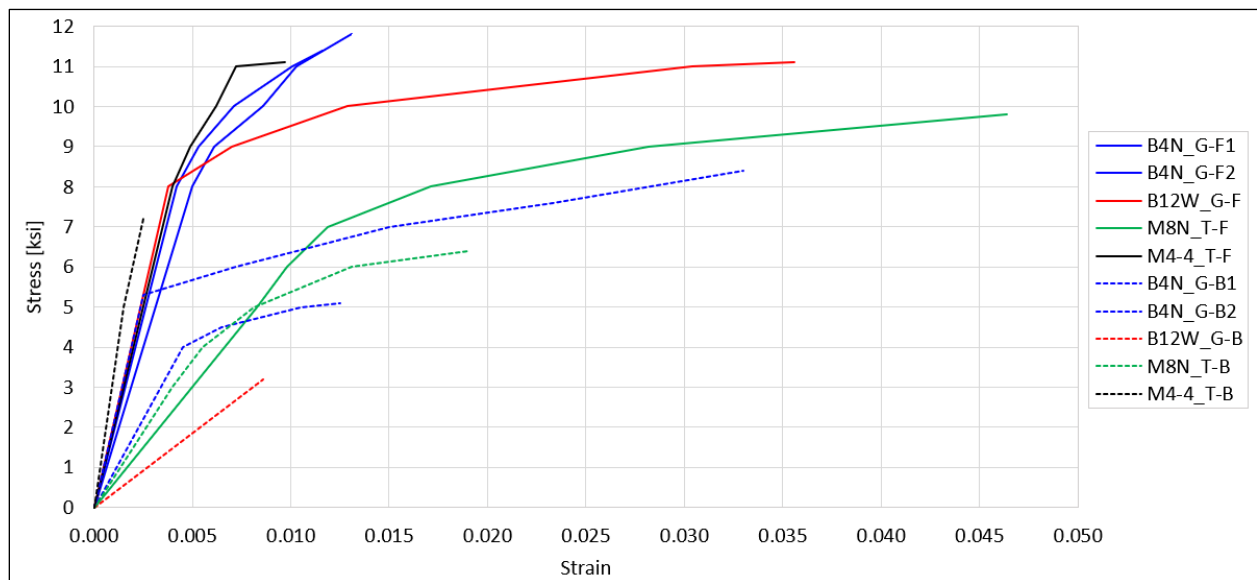


Figure 28: Strain-stress curves from tensile test results, up to ultimate stress.

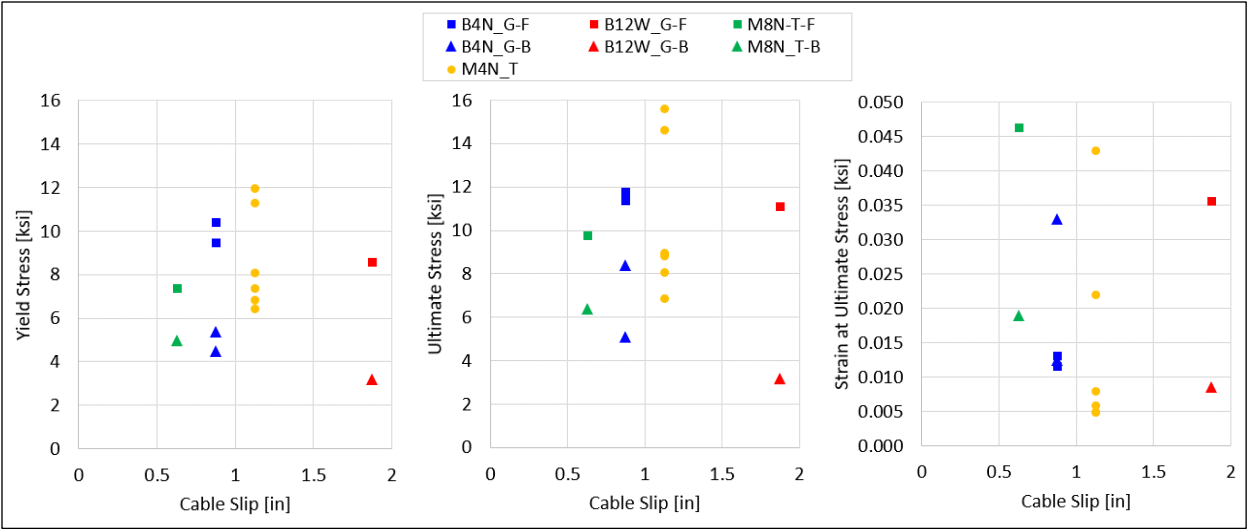


Figure 29: Zinc tensile test results vs. cable slip.

7.3 Grain Size

The zinc specimens cut from the socket castings and tested in tension were prepared for metallographic observation. The results are shown in Figure 30 to Figure 33, with each figure comparing the grain structure of the sample(s) taken at the front and back of a given casting. In every casting, the grains are smaller at the front of the casting and larger at the back. This is consistent with the tensile test results, where higher yield and ultimate tensile stresses were measured at the front of the casting. The smaller grain size is likely due to the faster cooling of the molten zinc at the front of the casting during the socketing process.

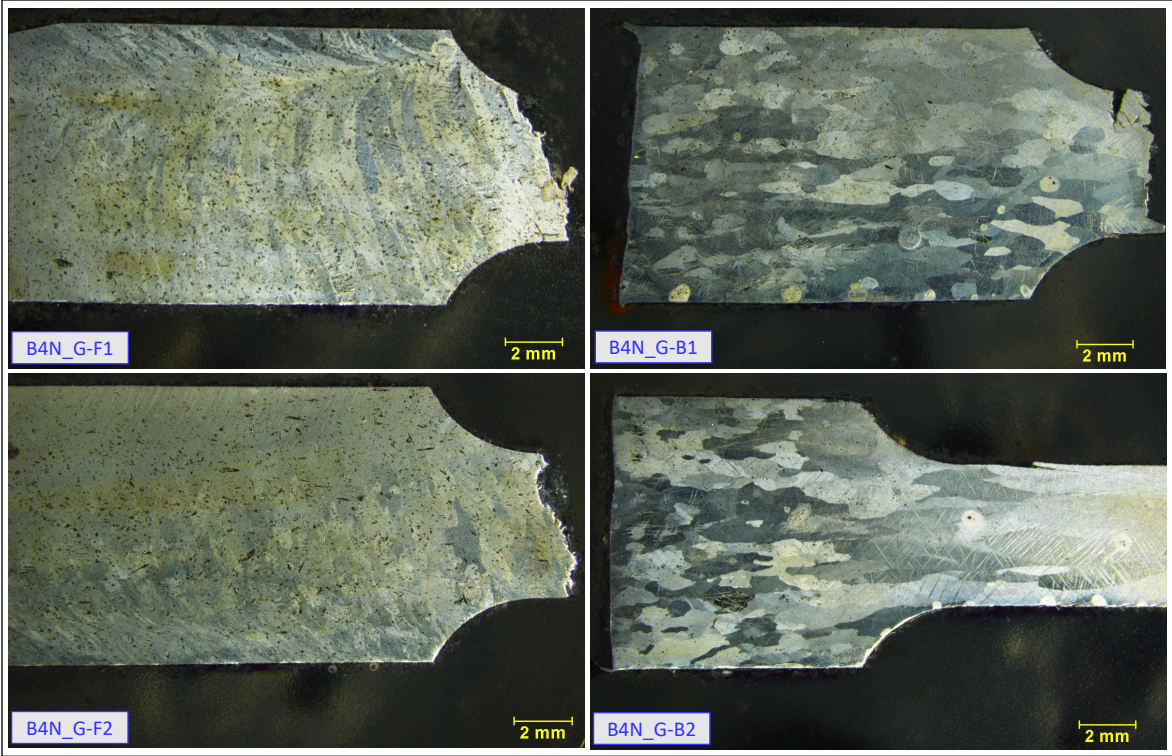


Figure 30: Grain size comparison between tensile specimens of socket B4N_G (photos: Socotec).

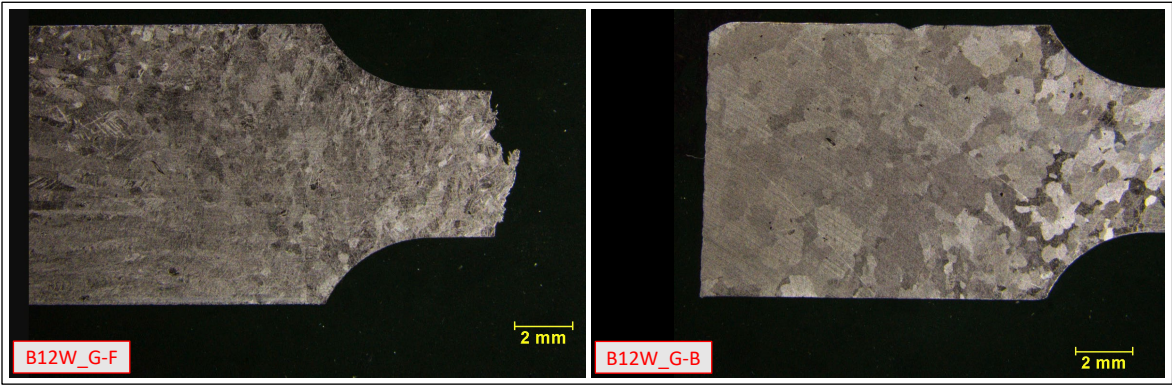


Figure 31: Grain size comparison between tensile specimens of socket B12W_G (photos: Socotec).

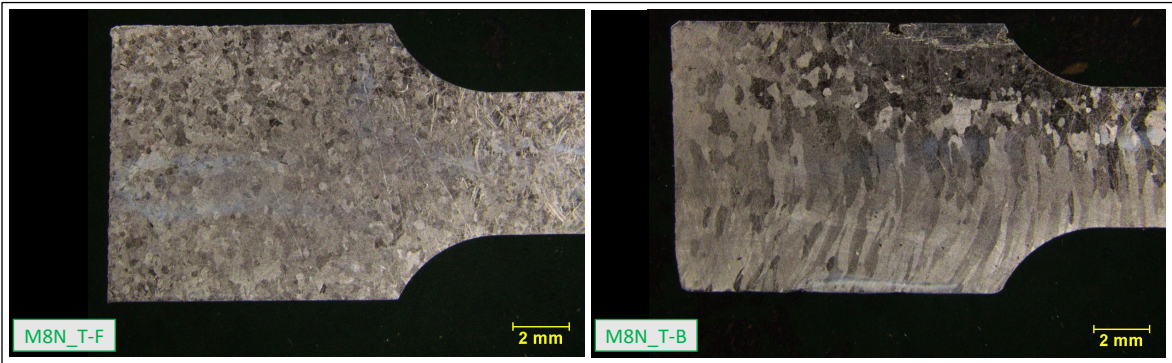


Figure 32: Grain size comparison between tensile specimens of socket M8N_T (photos: Socotec).

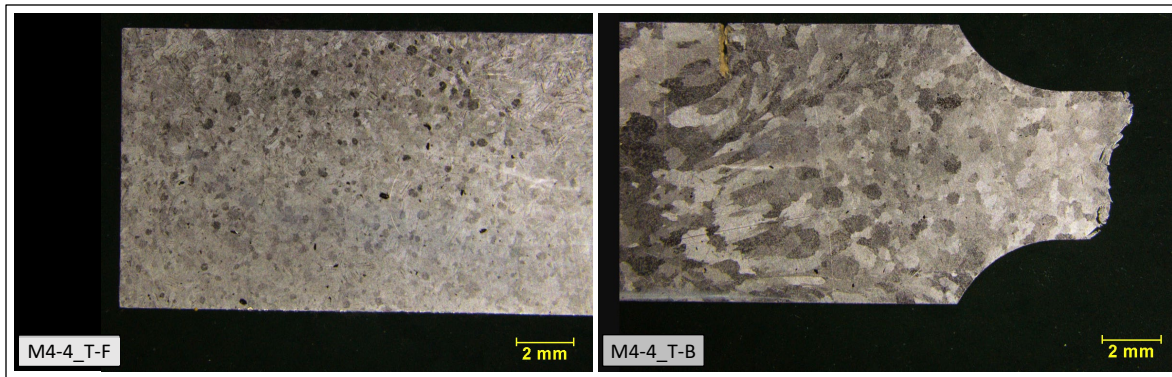


Figure 33: Grain size comparison between tensile specimens of socket M4-4_T (photos: Socotec).

8.0 Miscellaneous

8.1 No-Shoulder Socket Design

A socket is designed to terminate a cable of specific diameter, and to connect to the supporting structure with a specific detail. The six sockets considered in laboratory studies are of three different designs:

- Tower-end socket of original main cable: M4-4_T (failed November 6, 2020).
- Tower-end socket of auxiliary main cable: M4N_T (failed August 10, 2020) and M8N_T.
- Ground-end socket of auxiliary backstay cable: N4N_G, B4S_G and B12W_G (max. cable slip).

The laboratory studies revealed that these three socket designs featured a shoulder. As shown in Figure 34, the shoulder is a discontinuity in the slope of the socket's cavity near the front of the socket. However, as also shown in Figure 34, not all of the telescope's sockets had a shoulder design. The platform-end socket of an auxiliary main cable, M8N_P, was cut open by Socotec and found to not have a shoulder. The impact of the presence of a shoulder on the short-term and long-term behavior of the socket is studied in Appendix P.

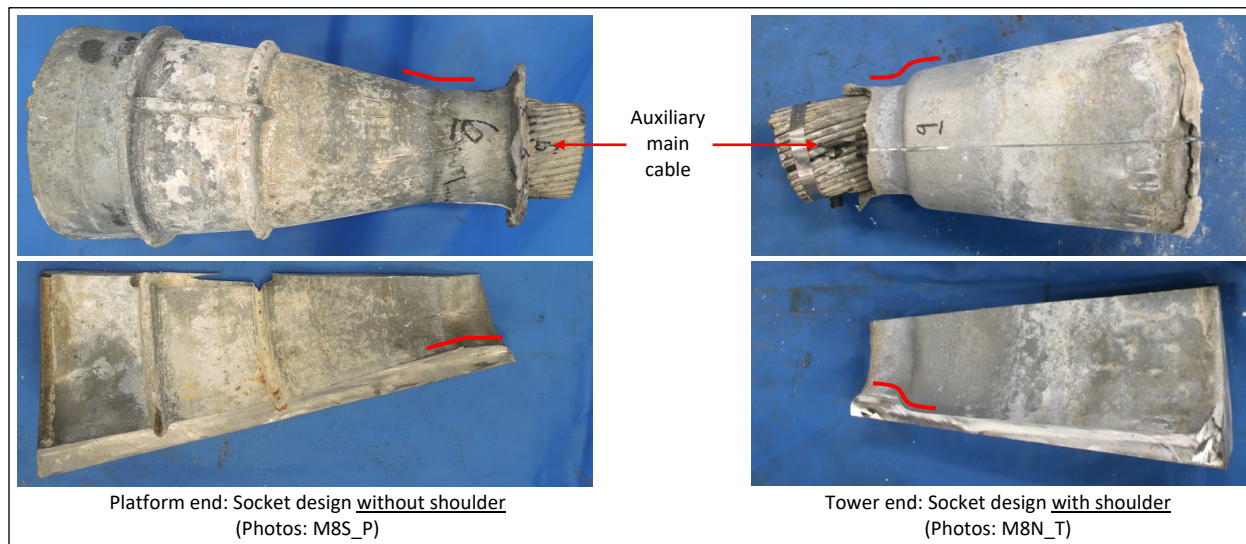


Figure 34: Socket designs with and without shoulder (photos: Socotec).

8.2 Wire Galvanizing Layer

The drawings specify the cables to be galvanized structural strands based on ASTM A586, class A which requires a minimum zinc coating weight of one ounce per square foot (equivalent to a thickness of 43 micrometer). During metallographic examination of the casting of socket B4N_G, it was observed that the zinc coating had not been removed from the wires prior to socketing (Figure 35). This observation is consistent with current socketing practice.

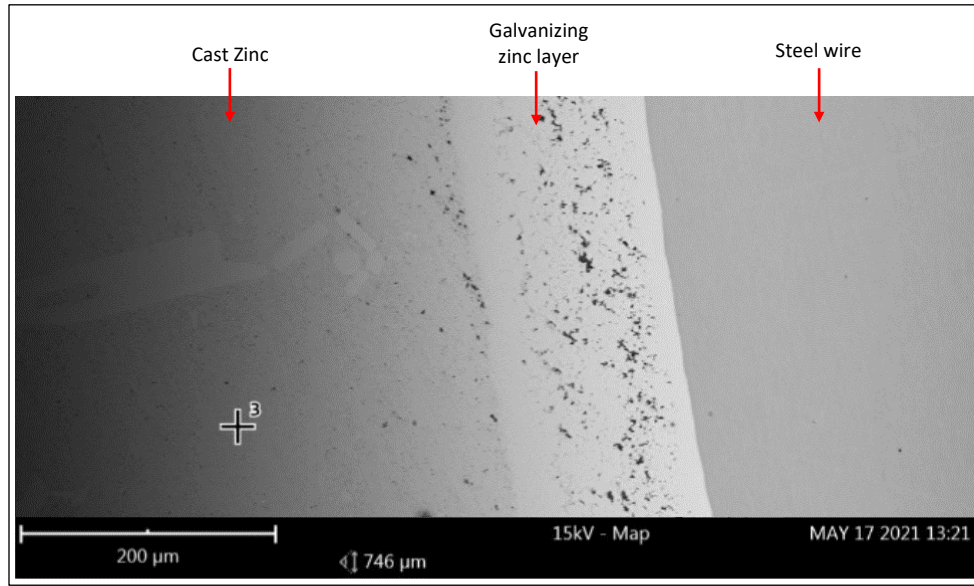


Figure 35: Galvanizing zinc layer on wires within zinc casting (photo: Socotec).